A local radial point interpolation method for dissipation process of excess pore water pressure

J.G. Wang
Tropical Marine Science Institute, National University of Singapore, Singapore
L. Yan
Institute of Mechanics, China Academy of Sciences, Beijing, People's Republic of China, and
G.R. Liu
Department of Mechanical Engineering, National University of Singapore, Singapore

Received August 2003
Revised September 2004
Accepted October 2004

Abstract

Purpose – Develop a local radial point interpolation method (LRPIM) to analyze the dissipation process of excess pore water pressure in porous media and verify its numerical capability.

Design/methodology/approach – Terzaghi's consolidation theory is used to describe the dissipation process. A local residual form is formulated over only a sub-domain. This form is spatially discretized by radial point interpolation method (RPIM) with basis of multiquadrics (MQ) and thin-plate spline (TPS), and temporally discretized by finite difference method. One-dimensional (1D) and two-dimensional consolidation problems are numerically analyzed.

Findings – The LRPIM is suitable, efficient and accurate to simulate this dissipation process. The shape parameters, $q = 1.03$, $R = 0.1$ for MQ and $\eta = 4.001$ for TPS, are still valid.

Research limitations/implications – The asymmetric system matrix in LRPIM spends more resources in storage and CPU time.

Practical implications – Local residual form requires no background mesh, thus being a truly meshless method. This provides a fast and practical algorithm for engineering computation.

Originality/value – This paper provides a simple, accurate and fast numerical algorithm for the dissipation process of excess pore water pressure, largely simplifies data preparation, shows that the shape parameters from solid mechanics are also suitable for the dissipation process.

Keywords Porous materials, Numerical analysis, Dissipation factor

Paper type Research paper

1. Introduction

Finite-element method has been widely used for the analysis of space-domain problems that have arbitrary shapes or complex geometries. It has been observed that the mesh generation is a far more time-consuming and expensive task than the assembly and solution of the finite-element equations. In order to avoid the mesh generation in finite-element method, meshless methods were proposed to avoid the connectivity among nodes. Great progress has been made in fluid mechanics (Kansa, 1990; Hon *et al.*, 1999), solid mechanics (Belytschko *et al.*, 1996; Atluri and Zhu, 1998; Wang and Liu, 2002a), soil mechanics (Murakami *et al.*, 2001; Wang *et al.*, 2002) and other applications

International Journal of Numerical Methods for Heat & Fluid Flow
Vol. 15 No. 6, 2005
pp. 567-587

0961-5539
DOI 10.1108/09615530510601468

(Wendland, 1999; Ho *et al.*, 2001; Singh *et al.*, 2003; Wang *et al.*, 2004) in recent years. Among meshless methods, radial point interpolation method (RPIM) (Wang and Liu, 2002a) is more attractive due to following characteristics. Firstly, point interpolation makes an approximation pass through each node within the problem domain, thus boundary conditions can be more easily implemented than the meshless methods based on moving least-square (MLS) approximation (Lancaster and Salkauskas, 1981; Belytschko *et al.*, 1996). Because the interpolation is based on a cluster of nodes instead of an element, the RPIM does not require the connectivity among nodes. This completely avoids the drawbacks of FEM. Secondly, shape functions and derivatives of the RPIM are explicitly expressed over a cluster of nodes only if radial basis functions (rbfs) are selected (Wang and Liu, 2002b). Thirdly, rbf maps multi-dimensional space into one-dimensional (1D) space. The smoothness of approximation can be easily determined in 1D space. Thus, the formulation based on the rbfs can be easily extended to higher dimensions. On this point, the meshless methods based on the rbfs are advantageous over the point interpolation method (PIM) based on only polynomial basis. This is because the singularity in the later is a big problem (Wang *et al.*, 2001). In fact, the MLS approximation also uses rbfs as weight function while only polynomials are used in basis functions. It is a mixed method of rbfs and polynomials. Finally, because the RPIM carries out the interpolation within each influence domain instead of global domain (Wang and Liu, 2002a, b), the system matrix obtained is sparse and banded, being more suitable for large-scale problems.

The RPIM is based on the global weak form which is developed over whole problem domain. Compared with collocation method such as references (Kansa, 1990; Zhang *et al.*, 2000; Hon *et al.*, 2002), this weak form has two advantages: lower order of derivatives and easier implementation of boundary conditions. However, the meshless methods based on the global weak form still requires background mesh for integration, thus RPIM is a pesudo-meshless method (Wang and Liu, 2002a). Collocation method directly discretizes partial differential equations with only scattered nodes within problem domain and on boundaries, thus being a true meshless method. However, this direct discretization requires higher order of derivatives and may have numerical oscillation (Zhang *et al.*, 2000). In order to take advantage of the weak form on lower derivatives and collocation method on only nodes (Larsson and Fornberg, 2003), a local residual formulation based on Petrov-Galerkin approach was proposed for MLS approximation (Atluri and Zhu, 1998). We combined the Petrov-Galerkin formulation with rbfs to formulate a local residual point interpolation (LRPIM) (Liu *et al.*, 2002) for solid mechanics problems. This LRPIM does not require any background mesh in the whole domain and is a true meshless method. This paper will extend the LRPIM to simulate the dissipation process of excess pore water pressure in porous media.

The dissipation process of excess pore water pressure in porous media can be described by Biot's consolidation theory (Wang *et al.*, 2002) where the deformation of porous medium interacts with the flow of pore water. The Mander-Cryer's effect at the initial stage of consolidation can be described in this theory. However, Biot's consolidation theory has complicated mathematical structure, thus both numerical and analytical solutions are not easily obtained. If the main characteristics of dissipation process are concerned, Terzaghi's consolidation theory is sufficient (Huang, 1983). Terzaghi consolidation theory assumes that total hydrostatic stress keeps constant during dissipation process. This largely simplifies the mathematical structure and its

solution procedure. This paper will solve two-dimensional (2D) Terzaghi's consolidation theory with LRPIM. This LRPIM uses rbfs for interpolation and local residual formulation for integration. It is still a weak-form based method, thus keeping all properties of weak-form types. Because only sub-domain is required for both interpolations and integrations, the nodes can be arbitrarily distributed within the problem domain. Therefore, the LRPIM is a true meshless method. This is advantageous over the RPIM as well as collocation methods.

This paper is organized as follows. Section 2 presents the formulation of Terzaghi's consolidation theory for multi-dimensional consolidation problems. Section 3 develops the local residual formulation for each node at each time step with weighted residual method. A quartic spline is proposed for the weight function. The excess pore water pressure is spatially discretized through RPIM and temporally discretized by finite difference method. The system equation is assembled through node-to-node approach. Section 4 presents the RPIM and the rbfs, multiquadric (MQ) (Hardy, 1990) and thin plate spline (TPS) (Powell, 1996), are incorporated into the LRPIM to form MQ-PIM and TPS-PIM, respectively. Section 5 checks the numerical performance of the LRPIM with 1D and 2D consolidation problems. The LRPIM results are compared with closed-form solution for 1D problem and FEM results for 2D problem. Conclusion is provided in Section 6.

2. Terzaghi's consolidation theory

Terzaghi's consolidation theory basically describes a dissipation process with a diffusion equation. It cannot give initial excess pore water pressure and deformation. This paper uses a two-step scheme to solve this issue. The first step is to solve a static elastic problem with undrained condition (Poisson ratio is used as 0.499 in computation). This step gets a stress distribution. Following empirical formulation is then employed to compute the initial excess pore water pressure at each node point within the problem domain Ω:

$$u_0 = B[\sigma_3 + A(\sigma_1 - \sigma_3)] \quad \text{in } \Omega \tag{1}$$

where A and B are material parameters of soil masses. $B = 1$ for saturated soils. $A = 1/3$ for linear elastic soils.

The second step is to numerically simulate the dissipation process of above initial excess pore water pressure by Terzaghi's consolidation theory. Terzaghi's consolidation theory can be developed from conservation law of soil masses and pore water. Darcy's law is assumed to be suitable for the seepage in porous media. For any element of the soil-water mixture, the flow-out of pore water is equal to the deformation of soil skeleton:

$$\frac{k_x}{\gamma_w}\frac{\partial^2 u}{\partial x^2} + \frac{k_y}{\gamma_w}\frac{\partial^2 u}{\partial y^2} + \frac{k_z}{\gamma_w}\frac{\partial^2 u}{\partial z^2} = -\frac{\partial \varepsilon_v}{\partial t} \quad \text{in } \Omega \tag{2}$$

where u is excess pore water pressure, k_x, k_y, k_z are the permeability of soil skeleton along x, y, z directions, respectively. γ_w is the water density. If soil skeleton is linearly elastic, ε_v, the volumetric strain of soil skeleton, is as follows for a three-dimensional

problem:

$$\varepsilon_v = \frac{1-2\nu}{E}(\Theta - 3u) \quad \text{in } \Omega \tag{3}$$

where $\Theta = \sigma_1 + \sigma_2 + \sigma_3$ is the total hydrostatic stress. Because Terzaghi's consolidation theory assumes this stress keeps constant during dissipation process, equation (3) becomes as:

$$\frac{\partial \varepsilon_v}{\partial t} = -\frac{3(1-2\nu)}{E}\frac{\partial u}{\partial t} \quad \text{in } \Omega \tag{4}$$

The Terzaghi's consolidation equation is obtained as:

$$\frac{k_x}{\gamma_w}\frac{\partial^2 u}{\partial x^2} + \frac{k_y}{\gamma_w}\frac{\partial^2 u}{\partial y^2} + \frac{k_z}{\gamma_w}\frac{\partial^2 u}{\partial z^2} = \frac{3(1-2\nu)}{E}\frac{\partial u}{\partial t} \quad \text{in } \Omega \tag{5}$$

It can be expressed as following general form:

$$C_{vxi}\frac{\partial^2 u}{\partial x^2} + C_{vyi}\frac{\partial^2 u}{\partial y^2} + C_{vzi}\frac{\partial^2 u}{\partial z^2} = \frac{\partial u}{\partial t} \quad (i = 1,2,3) \tag{6}$$

where the coefficient of consolidation along x-direction as an example is:

$$\begin{aligned} C_{vx3} &= \tfrac{k_x E}{3\gamma_w(1-2\nu)} && \text{for 3D problem} \\ C_{vx2} &= \tfrac{k_x}{2\gamma_w}\tfrac{E}{(1-2\nu)(1+\nu)} && \text{for 2D problem} \\ C_{vx1} &= \tfrac{k_x}{\gamma_w}\tfrac{E(1-\nu)}{(1-2\nu)(1+\nu)} && \text{for 1D problem} \end{aligned} \tag{7}$$

Boundary conditions:

$$\begin{aligned} u &= 0 && \text{for permeable boundary } \Gamma_u \\ \tfrac{\partial u}{\partial n} &= 0 && \text{for impermeable boundary } \Gamma_t \end{aligned} \tag{8}$$

Initial condition:

$$u|_{t=0} = u_0 \quad \text{in } \Omega \tag{9}$$

where n is the normal direction of boundary Γ_t.

3. Local residual formulation and discretization

3.1 Local residual formulation

A 2D problem as shown in Figure 1 is discussed. For convenience, the subscript "2" at the coefficient of consolidation is omitted hereafter. The Ω_s is a sub-domain within the problem domain Ω. It is the influence domain of dark dot node. All sub-domains should cover the Ω $\left(\Omega = \bigcup_s \Omega_s\right)$, and sub-domains must overlap each other ($\Omega_s \cap \Omega_l \neq \Phi$, Φ is empty set). We take a weight function W for this sub-domain Ω_s and let the weighted

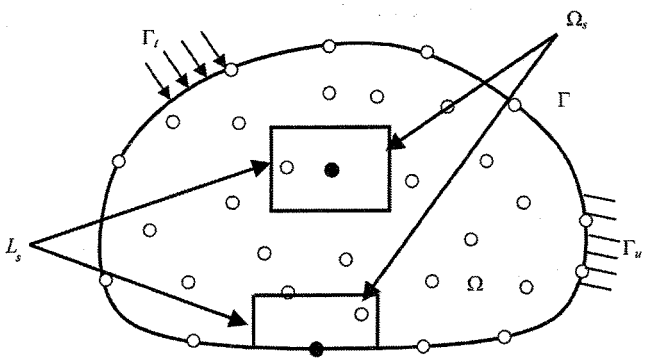

Figure 1.
A schematic description for local overlapping domain method

residual over the Ω_s equal to zero:

$$\int_{\Omega_s}\left(C_{vx}\frac{\partial^2 u}{\partial x^2}+C_{vy}\frac{\partial^2 u}{\partial y^2}-\frac{\partial u}{\partial t}\right)W\,dV=0 \tag{10}$$

Applying divergence theorem, equation (10) becomes:

$$\begin{aligned}&\int_{\Omega_s}\left(C_{vx}\frac{\partial u}{\partial x}\frac{\partial W}{\partial x}+C_{vy}\frac{\partial u}{\partial y}\frac{\partial W}{\partial y}\right)dV+\int_{\Omega_s}\frac{\partial u}{\partial t}W\,dV\\&-\int_{\partial\Omega_s}\left(C_{vx}\frac{\partial u}{\partial x}n_x+C_{vy}\frac{\partial u}{\partial y}n_y\right)W\,d\Gamma=0\end{aligned} \tag{11}$$

where $\partial\Omega_s = L_s + \Gamma_{su} + \Gamma_{st}$. L_s is the boundary of the sub-domain Ω_s. Γ_{su} and Γ_{st} are the parts of permeable and impermeable boundaries along the sub-domain boundary $\partial\Omega_s$. n_x, n_y are directional cosines along $\partial\Omega_s$. When the Ω_s locates entirely within the problem domain Ω, only L_s remains. Let the weight function W be zero along the internal boundary L_s, then equation (11) becomes:

$$\begin{aligned}&\int_{\Omega_s}\left(C_{vx}\frac{\partial u}{\partial x}\frac{\partial W}{\partial x}+C_{vy}\frac{\partial u}{\partial y}\frac{\partial W}{\partial y}\right)dV+\int_{\Omega_s}\frac{\partial u}{\partial t}W\,dV\\&-\int_{\Gamma_{st}}\left(C_{vx}\frac{\partial u}{\partial x}n_x+C_{vy}\frac{\partial u}{\partial y}n_y\right)W\,d\Gamma=0\end{aligned} \tag{12}$$

This is the local residual formulation or local weak form of Terzaghi's consolidation theory. Domain integration only concentrates on the sub-domain Ω_s. Interpolation point is usually the center or dark dot node and can be any point within the problem domain. Such localization largely avoids the element not only for interpolation but also for integration. It is a true meshless method.

3.2 Discretization within sub-domain

The discretization of excess pore water pressure is only done in sub-domain Ω_s. This Ω_s contains N nodes and the excess pore water pressure at the Ith node and time t is $u_I(t)$. The excess pore water pressure $u(\mathbf{x},t)$ at node $\mathbf{x}$ is approximately expressed by N nodal values:

$$u(\mathbf{x},t) = \sum_{I=1}^{N} \Phi_I(\mathbf{x}) u_I(t) \tag{13}$$

where $\Phi_I(\mathbf{x})$ is the shape function over the influence domain Ω_s. The partial derivatives of this approximation are then obtained as follows:

$$\begin{aligned} \frac{\partial u(\mathbf{x},t)}{\partial x} &= \sum_{I=1}^{N} \frac{\partial \Phi_I(\mathbf{x})}{\partial x} u_I(t) \\ \frac{\partial u(\mathbf{x},t)}{\partial y} &= \sum_{I=1}^{N} \frac{\partial \Phi_I(\mathbf{x})}{\partial y} u_I(t) \end{aligned} \tag{14}$$

$$\frac{\partial u(\mathbf{x},t)}{\partial t} = \sum_{I=1}^{N} \Phi_I(\mathbf{x}) \frac{\mathrm{d}u_I(t)}{\mathrm{d}t} \tag{15}$$

Equation (12) becomes the following differential equation after spatial discretization:

$$\mathbf{C}\frac{\mathrm{d}\omega(t)}{\mathrm{d}t} + \mathbf{K}\omega(t) = 0 \tag{16}$$

where

$$\begin{aligned} K_{ij} = &\int_{\Omega_s} \left(C_{vx} \frac{\partial \Phi_j(\mathbf{x})}{\partial x} \frac{\partial W(\mathbf{x},\mathbf{x}_i)}{\partial x} + C_{vy} \frac{\partial \Phi_j(\mathbf{x})}{\partial y} \frac{\partial W(\mathbf{x},\mathbf{x}_i)}{\partial y} \right) \mathrm{d}V \\ &- \int_{\Gamma_{st}} \left(C_{vx} \frac{\partial \Phi_j(\mathbf{x})}{\partial x} n_x + C_{vy} \frac{\partial \Phi_j(\mathbf{x})}{\partial y} n_y \right) W(\mathbf{x},\mathbf{x}_i)\, \mathrm{d}\Gamma \end{aligned} \tag{17}$$

$$C_{ij} = \int_{\Omega_s} \Phi_j(\mathbf{x}) W(\mathbf{x},\mathbf{x}_i)\, \mathrm{d}V \quad \omega(t) = [\, u_1(t) \quad u_2(t) \quad \cdots \quad u_N(t)\,]^{\mathrm{T}}$$

We use the following finite difference method to discretize the time domain in equation (16):

$$\int_t^{t+\Delta t} f(x)\, \mathrm{d}x = \Delta t[\theta f(t) + (1-\theta) f(t+\Delta t)] \tag{18}$$

Here $0 \leq \theta \leq 1$. A recursive form of equation (16) is obtained as:

$$\left(\frac{\mathbf{C}}{\Delta t} + \mathbf{K}(1-\theta)\right)\omega_{t+\Delta t} + \left(-\frac{\mathbf{C}}{\Delta t} + \mathbf{K}\theta\right)\omega_t = 0 \tag{19}$$

3.3 Weight function

Following quartic spline is used as weight function:

$$W(\mathbf{x}-\mathbf{x}_I) = \begin{cases} 1 - 6d^2 + 8d^3 - 3d^4 & d \leq 1 \\ 0 & d > 1 \end{cases} \tag{20}$$

where $d = |\mathbf{x} - \mathbf{x}_I|/r_I$ is the relative distance from node $\mathbf{x}_I$ to point $\mathbf{x}$, and r_I is the radius of sub-domain. This weight function is non-zero only within the influence domain Ω_s.

If the influence domain is taken as a rectangle of $n_d d_{xI} \times n_d d_{yI}$, where n_d is a scaling parameter and d_{xI}, d_{yI} the average distance between two neighboring nodes in the x-direction and the y-direction, respectively, the above weight function has the following form:

$$W(\mathbf{x}-\mathbf{x}_I) = W(r_x)\cdot W(r_y) = W_x \cdot W_y \tag{21}$$

where relative distances r_x and r_y are defined as:

$$r_x = \frac{|x - x_I|}{n_d \cdot d_{xI}}, \quad r_y = \frac{|y - y_I|}{n_d \cdot d_{yI}} \tag{22}$$

3.4 Numerical procedure

The numerical procedure or flowchart is listed as follows:

(1) Determine time step

(2) Loop over node points
- Determine the domain of influence for specified node and select neighboring nodes based on a predefined criterion such as rectangle.
- Compute shape function and its derivatives for each node point.
- Evaluate stiffness and loading at each node point within sub-domain.
- Assemble the contribution of each node to nodes system equation.

(3) End node point loop

(4) Introduce permeable boundary condition through modification of system equation by the method in Wang *et al.* (2004)

(5) Solve the system equation to obtain the excess pore water pressure at each node

(6) Forward to next time step until end criterion.

4. Radial PIM interpolation

4.1 Point interpolation method

The shape function Φ_I within an influence domain can be constructed through RPIM (Wang and Liu, 2002a, b). The influence domain Ω_s for point $\mathbf{x}$, where excess pore water pressure is $u(\mathbf{x})$, has N nodes at which the excess pore water pressures are $u_I (I = 1, 2, \ldots, N)$. This $u(\mathbf{x})$ can be approximated as:

$$u(\mathbf{x}) = \sum_{I=1}^{N} B_I(\mathbf{x}) a_I = \mathbf{B}^{\mathrm{T}}(\mathbf{x})\mathbf{a} \tag{23}$$

where the coefficient vector $\mathbf{a}$ and basis function $B_I(\mathbf{x})$ are as follows:

$$\mathbf{a}^{\mathrm{T}} = [a_1 \quad a_2 \quad \ldots \quad a_N], \quad B_I(\mathbf{x}) = B_I(r) \tag{24}$$

where r is the distance between point $\mathbf{x}$ and node $\mathbf{x}_I$. In 2D space

$$r = \left[(x - x_I)^2 + (y - y_I)^2\right]^{\frac{1}{2}} \tag{25}$$

Let the approximation of equation (23) pass through all N nodes within the influence domain:

$$\sum_{I=1}^{N} a_I B_I(r_k) = u_k \quad k = 1, 2, \ldots, N \tag{26}$$

where $r_k = \left[(x_k - x_I)^2 + (y_k - y_I)^2\right]^{\frac{1}{2}}$

Therefore, the coefficient $\mathbf{a}$ is uniquely determined as follows:

$$\mathbf{a} = \mathbf{B}_0^{-1}\mathbf{u} \tag{27}$$

where

$$\mathbf{u}^{\mathrm{T}} = [u_1 \quad u_2 \quad \ldots \quad u_N] \quad \mathbf{B}_0 = \begin{bmatrix} B_1(r_1) & B_2(r_1) & \ldots & B_N(r_1) \\ B_1(r_2) & B_2(r_2) & \ldots & B_N(r_2) \\ \ldots & \ldots & \ldots & \ldots \\ B_1(r_N) & B_2(r_N) & \ldots & B_N(r_N) \end{bmatrix} \tag{28}$$

The approximation function $u(\mathbf{x})$ is finally obtained as

$$u(\mathbf{x}) = \mathbf{B}^{\mathrm{T}}(r)\mathbf{B}_0^{-1}\mathbf{u} = \Phi(\mathbf{x})\mathbf{u} \tag{29}$$

where $\Phi(\mathbf{x}) = \mathbf{B}^{\mathrm{T}}(r)\mathbf{B}_0^{-1}$ is the shape function, and $\mathbf{B}^{\mathrm{T}}(r) = [\mathbf{B}_1(r) \; B_2(r) \; \ldots \; B_N(r)]$. The shape function depends uniquely on the distribution of scattered nodes within the influence domain. The partial derivatives of approximation function are:

$$\frac{\partial u}{\partial x} = \begin{bmatrix} \frac{\partial B_1}{\partial x} & \frac{\partial B_2}{\partial x} & \ldots & \frac{\partial B_N}{\partial x} \end{bmatrix} \mathbf{B}_0^{-1}\mathbf{u} \quad \frac{\partial u}{\partial y} = \begin{bmatrix} \frac{\partial B_1}{\partial y} & \frac{\partial B_2}{\partial y} & \ldots & \frac{\partial B_N}{\partial y} \end{bmatrix} \mathbf{B}_0^{-1}\mathbf{u} \tag{30}$$

Above PIM has two attractive features. The first is that the shape functions are of Kronecker Delta properties. This makes the implementation of permeable boundary conditions much easier than MLS approximation. The second is that the inverse of $\mathbf{B}_0$ is available for almost any distribution of scattered nodes, thus no special treatment is necessary to avoid the singularity problem (Wang *et al.*, 2001).

4.2 Radial basis functions

Two typical rbfs, multiquadric (MQ) and thin-plate spline (TPS) are used in computation. The MQ basis function has the following form:

$$B_I(x,y) = \left(r_I^2 + R^2\right)^q \tag{31}$$

where q and R are shape parameters. The derivatives of MQ basis function are:

$$\frac{\partial B_I}{\partial x} = 2q\left(r_I^2 + R^2\right)^{q-1}(x - x_I) \quad \frac{\partial B_I}{\partial y} = 2q\left(r_I^2 + R^2\right)^{q-1}(y - y_I) \tag{32}$$

The TPS basis function has the form as:

$$B_I(x,y) = r_I^\eta \tag{33}$$

where η is a shape parameter. The derivatives of the TPS basis function are:

$$\frac{\partial B_I}{\partial x} = \eta r_I^{\eta-1}(x - x_I) \quad \frac{\partial B_I}{\partial y} = \eta r_I^{\eta-1}(y - y_I) \tag{34}$$

For convenience, MQ-PIM and TPS-PIM denote the combination of LRPIM with MQ and TPS, respectively.

5. Numerical performance

The consolidation process of a foundation subject to surface loading is studied. As shown in Figure 2, the thickness of soil layer is $H = 16$ m. A width of 48 m is taken to form a computational domain. The boundary conditions are as follows: two sides and bottom are impermeable and the upper surface is permeable. If a uniform load is full of top surface as shown in Figure 2(a), this is a typical Terzaghi's consolidation problem. If only partial load is applied onto the surface as shown in Figure 2(b), this is a 2D problem. Foundation soil is linearly elastic with Young's modulus $E = 4.0 \times 10^4$ kPa, Poisson ratio $\nu = 0.3$, and the isotropic permeability $k_x = k_y = k = 1.728 \times 10^{-3}$ m/day (2×10^{-8} m/s). Two types of node distributions, regular in Figure 3(a) which has 833 nodes and irregular in Figure 3(b) which has 820 nodes, are used to study the effect of node distributions. Based on our previous study (Wang and Liu, 2002b; Liu *et al.*, 2002), the shape parameters are taken as $q = 1.03$, $R = 0.1$ for MQ-PIM and $\eta = 4.001$ for TPS-PIM. The influence domain is rectangle and the scaling parameter is taken as $n_d = 2.0$.

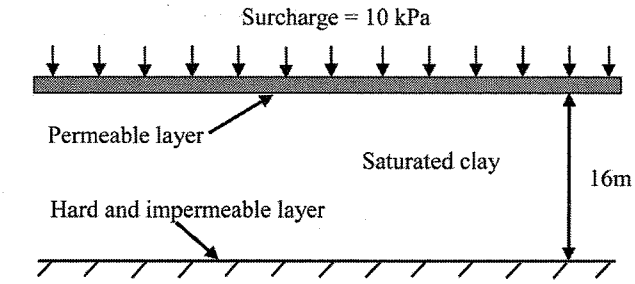

(a) One-dimensional consolidation model

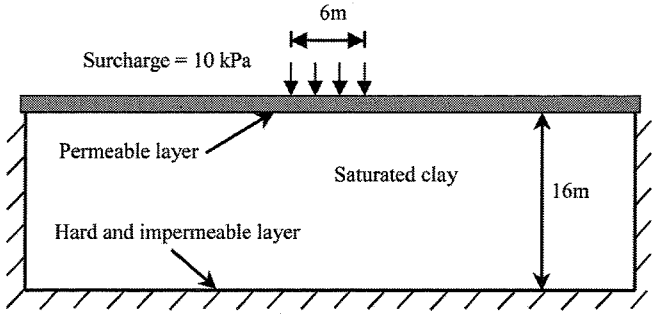

(b) Two-dimensional consolidation model

Figure 2.
Consolidation problems for 1D and 2D cases

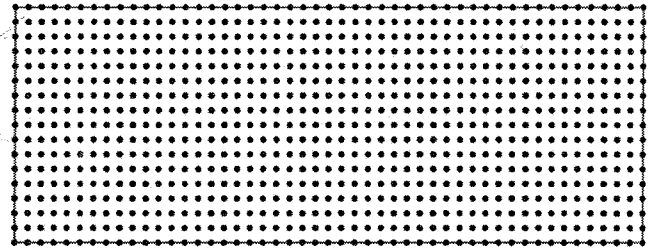

(a) Regular node distribution (833 nodes)

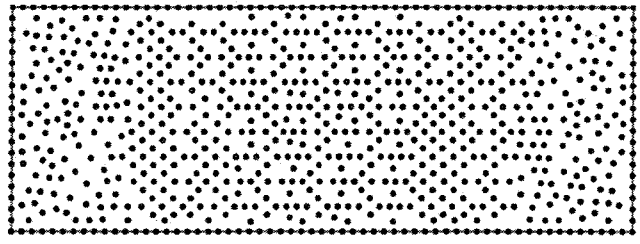

(b) Irregular node distribution (820 nodes)

Figure 3.
Meshless models for 1D and 2D problems

5.1 One-dimensional consolidation problem

The top surcharge is taken as $\Delta\sigma = 10\,\text{kPa}$ for 1D consolidation problem (Figure 2(a)). This problem has a closed-form solution:

$$u = \frac{4}{\pi}\Delta\sigma\sum_{n=1}^{\infty}\frac{1}{2n-1}\sin\left(\frac{(2n-1)\pi y}{2H}\right)e^{-(2n-1)^2\frac{\pi^2}{4}T_v} \tag{35}$$

The surface settlement S_t is

$$S_t = m_v\Delta\sigma H\left(1 - \frac{8}{\pi^2}\sum_{n=1}^{\infty}\frac{1}{(2n-1)^2}e^{-(2n-1)^2\frac{\pi^2}{4}T_v}\right) \tag{36}$$

where

$$T_v = \frac{C_{v1}}{H^2}t, \quad m_v = \frac{(1+\nu)(1-2\nu)}{E(1-\nu)}.$$

The surface settlement is numerically computed as

$$S_t^{\text{num}} = m_v\left(\Delta\sigma H - \int_0^H u\,dy\right) \tag{37}$$

It is noted that 1D problem has no immediate deformation after loading. Therefore, initial surface settlement is zero. We take $\theta = 0.5$ and the time step Δt is taken between 5×10^3 and 6×10^4 s to ensure numerical stability. Figure 4 gives the sampling points 4, 9 and 14 for comparison.

For 1D problem, initial excess pore water pressure is equal to surcharge everywhere. For comparison, FEM analysis is also carried out with quadrilateral elements for regular node distribution (833 nodes). Figure 5 compares the excess pore water pressures obtained by MQ-PIM, closed-form solution and FEM, and Figure 6 compares the results obtained by TPS-PIM, closed-form solution and FEM. The results by FEM and LRPIM agree well at the three sampling points. However, some difference is observed between closed-form solution and numerical results. The effect of node distributions is also studied. Figure 7(a) compares the surface settlements obtained by

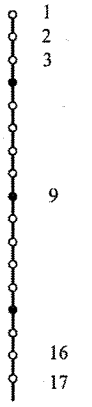

Depth of selected points along central line

Point number	y-coordinate (m)
4	3
9	8
14	13

Figure 4.
Sample points and coordinates

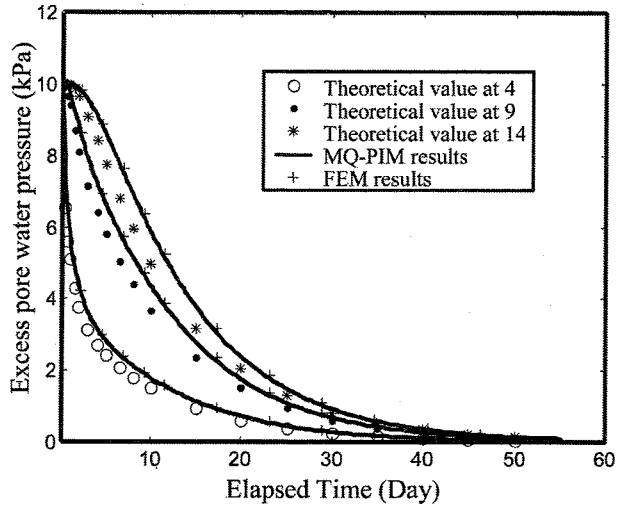

(a) Regular node distribution

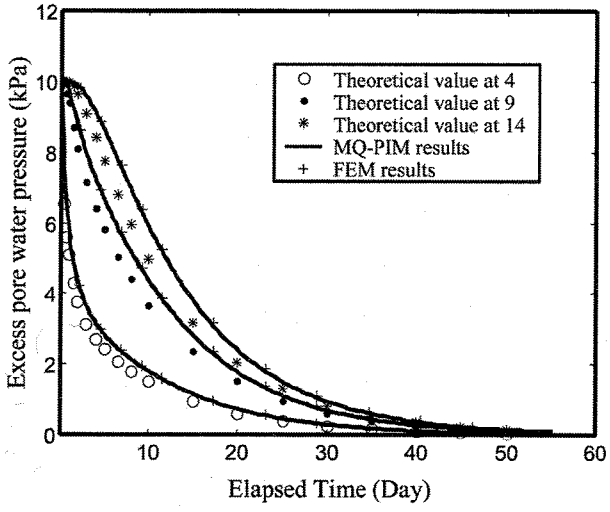

(b) Irregular node distribution

Figure 5.
Comparison of excess pore water pressure for MQ basis

closed-form solution and MQ-PIM for regular and irregular node distributions. Figure 7(b) is the comparison for TPS-PIM. Both MQ-PIM and TPS-PIM are not sensitive to node distributions. This is one of the advantages over the PIM with polynomial basis. The surface settlement of LRPIM is a little lower than that of closed-form solution, which is consistent with the slower dissipation process of excess pore water pressure. As a general, the numerical results by both MQ-PIM and TPS-PIM are acceptable. Figure 8 is a typical spatial distribution of excess pore water

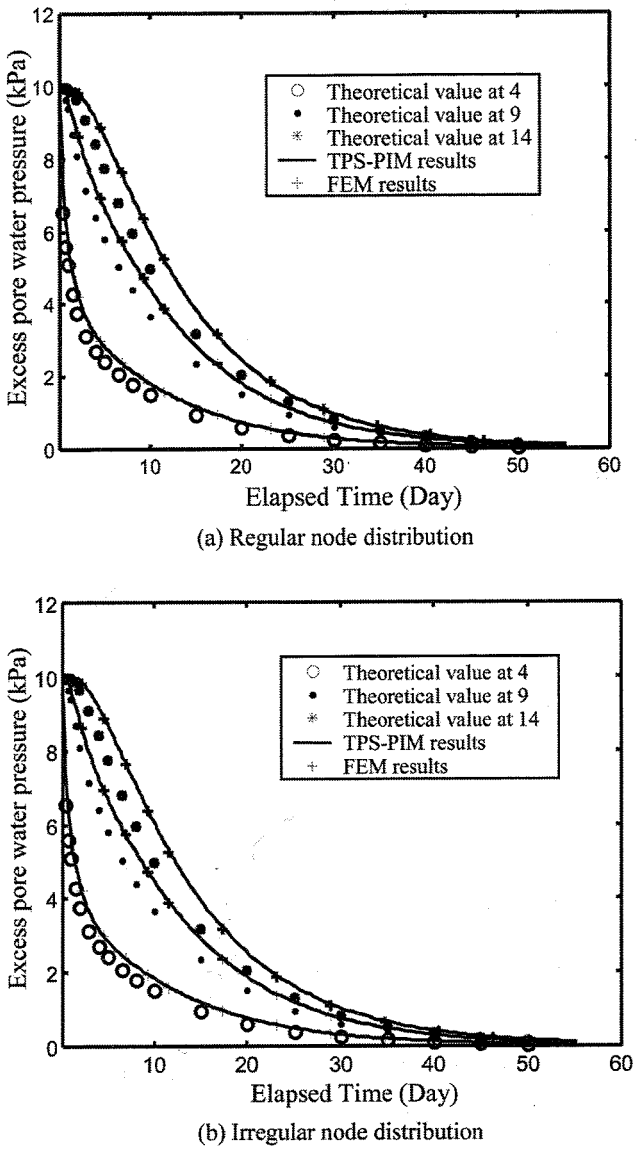

(a) Regular node distribution

(b) Irregular node distribution

Figure 6.
Comparison of excess pore water pressure for TPS basis

pressure at different times, which is similar to the results calculated by Biot's consolidation theory (Wang *et al.*, 2001). Oscillation of excess pore water pressure is not observed at the early stage of consolidation process (Wang *et al.*, 2002). From this simple example, it can be concluded that the LRPIM is not sensitive to node distributions, and both MQ-PIM and TPS-PIM can achieve reasonable accuracy for 1D Terzaghi's consolidation problem.

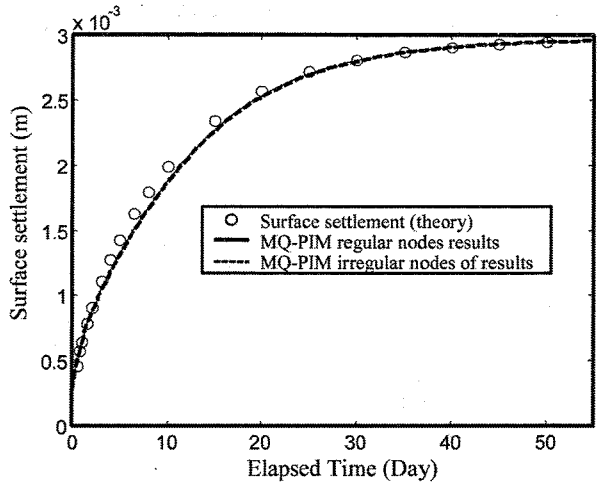

(a) MQ-PIM

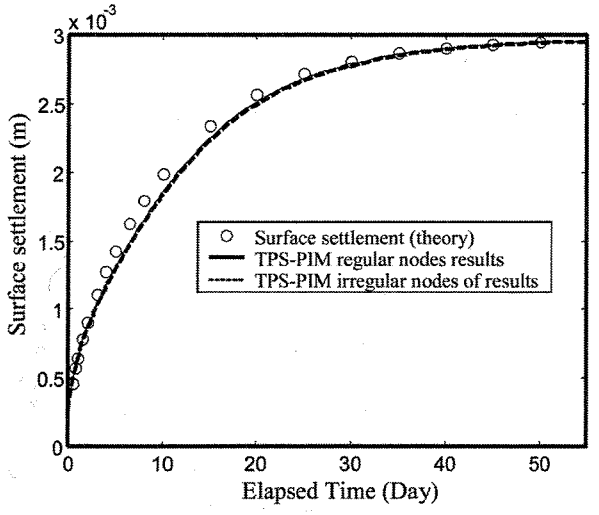

(b) TPS-PIM

Figure 7.
Comparison of surface settlement for different node distributions

5.2 Two-dimensional consolidation problem

5.2.1 Initial excess pore water pressure. A strip load is applied onto the top surface as shown in Figure 2(b). We use the same soil parameters as the 1D problem. Being different from the 1D problem, the stress distribution within the problem domain should be computed by an undrained static problem. After obtaining the stress distribution, the initial excess pore water pressure at each node is determined by equation (1). For the undrained static problem, we use the Poisson ratio of 0.499. In computation, care must be taken for the integration over volumetric term and reduction

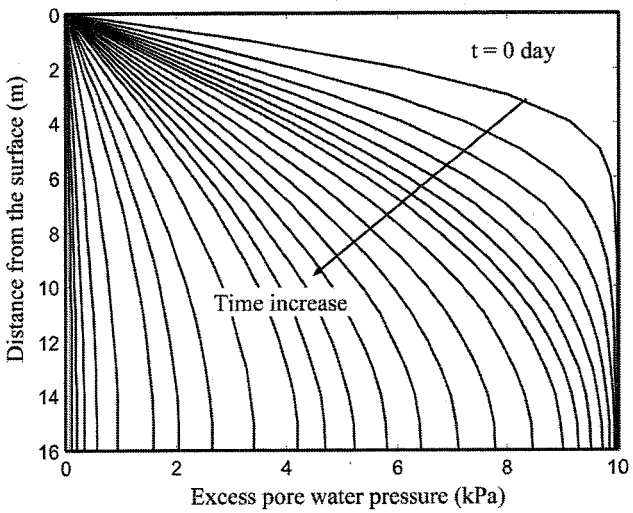

Figure 8.
Distribution of excess pore water pressure at different time

integration is a good choice if necessary (Wang *et al.*, 2003). Figure 9 is the contour of the initial pore water pressure. This pore water pressure is input into above LRPIM program, and the dissipation process of excess pore water pressure is simulated.

5.2.2 Comparison of LRPIM with FEM. We have compared the results obtained by LRPIM and FEM for 1D problem, and found that the LRPIM results agree well with FEM. This section continues the comparison for 2D problems. Regular node distribution (833 nodes) is used for both LRPIM and FEM. FEM uses the quadrilateral elements while LRPIM uses the same parameters as 1D problem. Figure 10 compares the excess pore water pressures computed by LRPIM and FEM at three sampling points. Figure 10(a) is for MQ-PIM and Figure 10(b) is for TPS-PIM. In the whole dissipation process, both MQ-PIM and TPS-PIM agree well with FEM. The accuracy of both MQ-PIM and TPS-PIM is comparable to FEM for this problem.

5.2.3 Effect of node irregularity. The effect of node irregularity is shown in Figure 11. Figure 11(a) compares the dissipation process obtained by MQ-PIM and Figure 11(b) is the comparison for TPS-PIM. A little difference is observed at the initial excess pore water pressure. This is caused by the static problem. However, this difference does reduce with the dissipation process of excess pore water pressure. These numerical results are not, in general, sensitive to node distributions at the dissipation process.

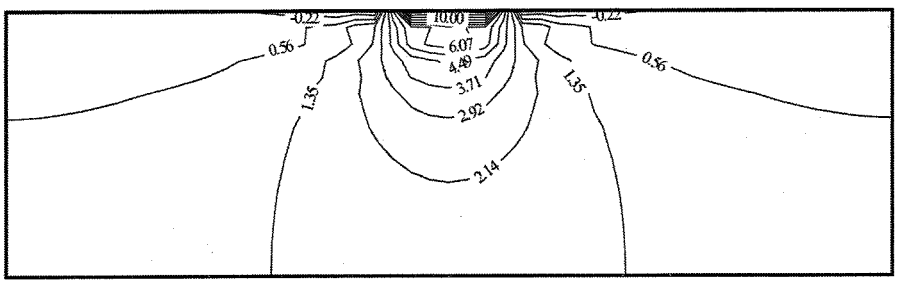

Figure 9.
Initial excess pore water pressure for 2D problem

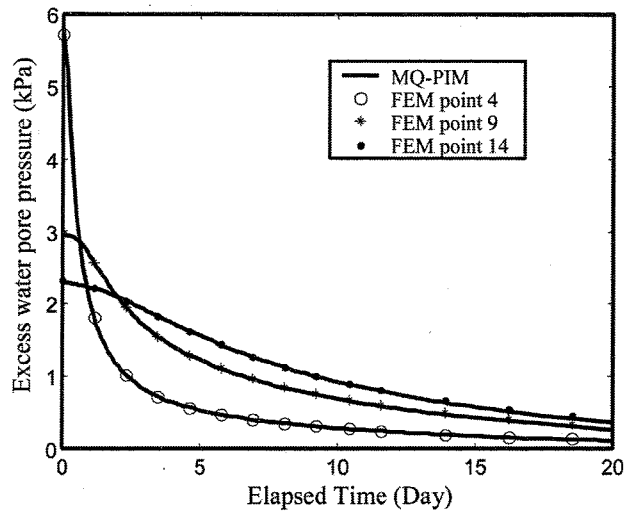

(a) MQ-PIM

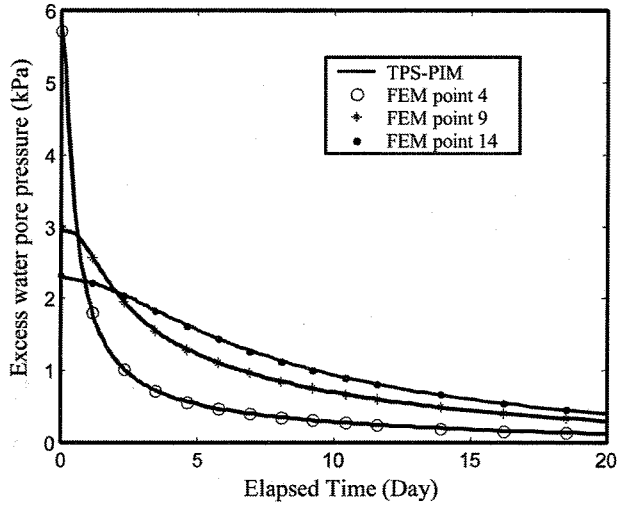

(b) TPS-PIM

Figure 10.
Dissipation process of excess pore water pressure for 2D problem ($\nu = 0.3$)

Therefore, the LRPIM is not sensitive to node distributions. This is an important advantage of the LRPIM over the PIM with polynomial basis.

5.2.4 Effect of Poisson ratios. Poisson ratio is an important parameter. We calculate the dissipation process when Poisson ratios are $\nu = 0.0$ and 0.45. The same problem is also computed by FEM. A typical result is shown in Figure 12 for TPS-PIM. These figures show that lower Poisson ratio produces lower rate of dissipation. For example, at the 20th day, excess pore water pressure almost completely dissipates for the Poisson

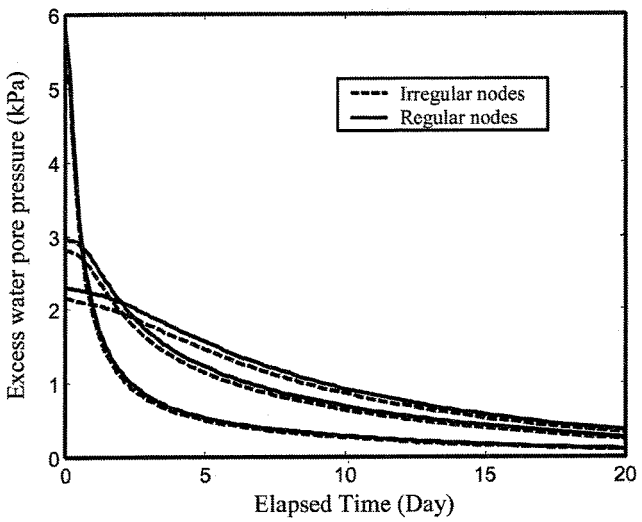

(a) MQ-PIM

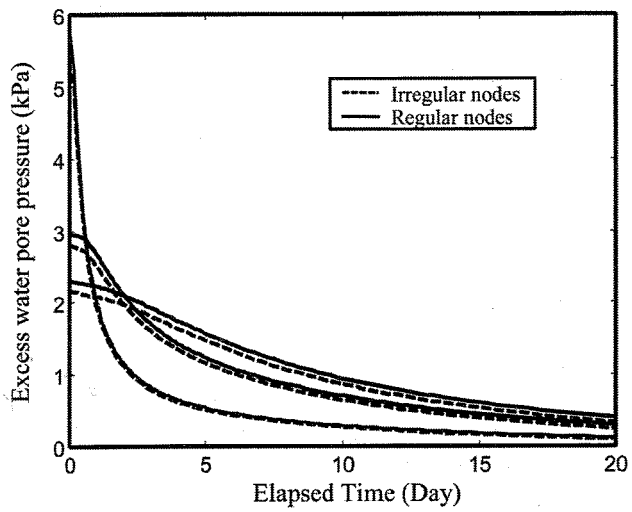

(b) TPS-PIM

Figure 11.
Effect of node irregularity on excess pore water pressure (2D problem and $\nu = 0.3$)

ratio of 0.45, while residual excess pore water pressure is still high for the Poisson ratio of 0.0.

5.2.5 Effect of permeability anisotropy. The permeability in x-direction is assumed to be three times of that in y-direction. We take $k_y = k$ in computation. All other parameters are the same as above 2D problem. MQ-PIM and regular node distribution are used. Figure 13(a) shows the effect of permeability anisotropy on the dissipation process of excess pore water pressure and Figure 13(b) is the contours of pore water

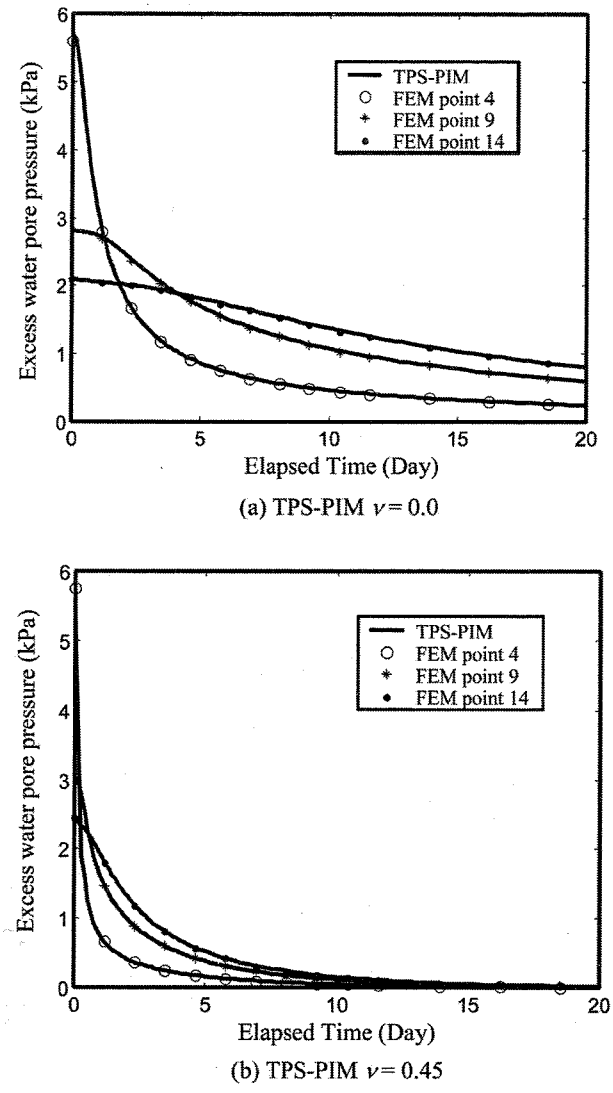

Figure 12.
Effect of Poisson ratios on dissipation of excess pore water pressure (2D problem)

pressure at the time 1 day. The anisotropic soil dissipates faster than the isotropic soil because the horizontal layer is a good seepage passage.

6. Conclusion

A local radial point interpolation method (LRPIM) was presented and applied to the dissipation process of excess pore water pressure in this paper. A residual formulation was developed based on the sub-domain within the problem domain and quartic spline was used as weight function. Excess pore water pressure was discretized through RPIM. Multiquadrics (MQ) and TPS are employed to form the MQ-PIM and TPS-PIM.

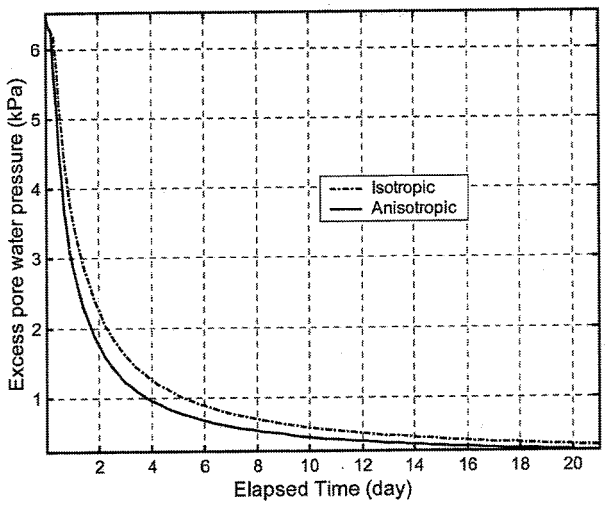

(a) Dissipation process at central line point below surface 2m

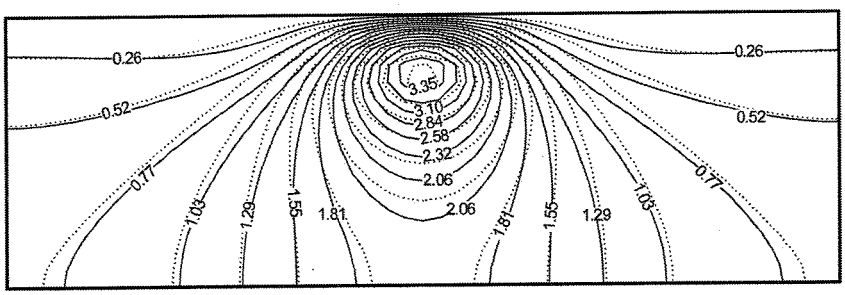

(b) Contour of excess pore water pressure at 1 day (solid line: isotropic; dot line: anisotropic)

Figure 13.
Effect of permeability anisotropy on dissipation of excess pore water pressure

Finally these MQ-PIM and TPS-PIM are used to study 1D and 2D consolidation problems. The results are compared with either closed-form solution or FEM results. Based on this study, following conclusions can be made:

First, the RPIM overcomes the drawbacks of MLS approximation such as the complexity in shape functions and difficulty in the implementation of permeable boundary conditions. It also avoids the singularity of PIM using only polynomial basis. Furthermore, the RPIM has the same formulation for both 1D and multi-dimensional problems.

Second, the LRPIM is advantageous over both collocation method and RPIM. It requires lower order of derivatives and less cost to implement boundary conditions than collocation method. The local non-zero weight function localizes the integration just over an influence domain, thus avoiding the background mesh over whole problem domain. The LRPIM is true meshless for both interpolation and integration, thus being advantageous over the RPIM.

Third, MQ-PIM and TPS-PIM are efficient and accurate to solve the diffusion equation of Terzaghi consolidation theory. Numerical results are not sensitive to node

distributions, dimensions and soil parameters. Because the Terzaghi's consolidation theory does not include an initial excess pore water pressure, a static problem has to be solved before dissipation process. This static problem may cause large error for the initial distribution of excess pore water pressure when Poisson ratio approaches to 0.5. Special care has to be taken to treat the volumetric integration for this static problem.

References

Atluri, S.N. and Zhu, T.A. (1998), "A new meshless local Petrov-Galerkin (MLPG) approach in computational mechanics", *Computational Mechanics*, Vol. 22, pp. 117-27.

Belytschko, T., Krongauz, Y., Organ, D., Fleming, M. and Krysl, P. (1996), "Meshless methods: an overview and recent developments", *Comput. Methods Appl. Mech. Eng.*, Vol. 139, pp. 3-47.

Hardy, R.L. (1990), "Theory and applications of the multiquadrics – Biharmonic method (20 years of discovery 1968-1988)", *Computers and Mathematics with Applications*, Vol. 19, pp. 163-208.

Ho, S.L., Yang, S., Machado, J.M. and Wong, H.C. (2001), "Application of a meshless method in electromagnetics", *IEEE Transactions on Magnetics*, Vol. 37 No. 5, pp. 3198-202.

Hon, Y.C., Cheung, K.F., Mao, X.Z. and Kansa, E.J. (1999), "A multiquadric solution for the shallow water equations", *Journal of Hydraulic Engineering, ASCE*, Vol. 125 No. 5, pp. 524-33.

Hon, Y.C., Lu, M.W., Xue, M.W. and Zhou, X. (2002), "Numerical algorithm for triphasic model of charged and hydrated soft tissues", *Computational Mechanics*, Vol. 29 No. 1, pp. 1-15.

Huang, W.X. (1983), *Engineering Properties of Soils* (in Chinese), Hydraulic and Electric Publishing Press, Beijing.

Kansa, E.J. (1990), "Multiquadrics – a scattered data approximation scheme with applications to computational fluid mechanics – I & II", *Computers and Mathematics with Applications*, Vol. 19, pp. 127-61.

Lancaster, P. and Salkauskas, K. (1981), "Surfaces generated by moving least squares methods", *Math. Comput.*, Vol. 37, pp. 141-58.

Larsson, E. and Fornberg, B. (2003), "A numerical study of some radial basis function based solution methods for elliptic PDEs", *Computers and Mathematics with Applications*, Vol. 46 Nos 5/6, pp. 891-902.

Liu, G.R., Yan, L., Wang, J.G. and Gu, Y.T. (2002), "Point interpolation method based on local residual formulation using radial basis functions", *Structural Engineering and Mechanics*, Vol. 14 No. 6, pp. 713-32.

Murakami, A., Kawabata, H. and Aoyama, S. (2001), "EFGM analysis for saturated soils", in Desai, C.S., *et al.* (Eds), *Computer Methods and Advances in Geomechanics*, 1, pp. 153-6.

Powell, M.J.D. (1996), "A review of algorithms for thin plate spline interpolation in two dimensions", in Fontanella, F., Jetter, K. and Laurent, P.J. (Eds), *Advanced Topics in Multivariate Approximations*, pp. 303-22.

Singh, I.V., Sandeep, K. and Prakash, R. (2003), "Heat transfer analysis of two-dimensional fins using a meshless element free Galerkin method", *Numerical Heat Transfer*, Vol. 44, Part A, pp. 73-84.

Wang, J.G. and Liu, G.R. (2002a), "A point interpolation meshless method based on radial basis functions", *International Journal for Numerical Methods in Engineering*, Vol. 54 No. 11, pp. 1623-48.

Wang, J.G. and Liu, G.R. (2002b), "On the optimal shape parameters of radial basis functions used for 2-D meshless methods", *Computer Methods in Applied Mechanics and Engineering*, Vol. 191 Nos 23/24, pp. 2611-30.

Wang, J.G., Liu, G.R. and Lin, P. (2002), "Numerical analysis of Biot's consolidation process by radial point interpolation method", *International Journal of Solids and Structures*, Vol. 39 No. 6, pp. 1557-73.

Wang, J.G., Liu, G.R. and Wu, Y.G. (2001), "A point interpolation method for simulating dissipation process of consolidation", *Computer Methods in Applied Mechanics and Engineering*, Vol. 190 No. 45, pp. 5907-22.

Wang, J.G., Leung, C.F. and Chow, Y.K. (2003), "Numerical solutions for flow in porous media", *International Journal for Numerical and Analytical Methods in Geomechanics*, Vol. 27 No. 7, pp. 565-83.

Wang, J.G., Zhang, B.Y. and Nogami, T. (2004), "Wave-induced seabed response analysis by radial point interpolation meshless method", *Ocean Engineering*, Vol. 31 No. 1, pp. 21-42.

Wendland, H. (1999), "Meshless Galerkin method using radial basis functions", *Mathematics of Computation*, Vol. 68 No. 228, pp. 1521-31.

Zhang, X., Song, K.Z. and Lu, M.W. (2000), "Meshless methods based on collocation with radial basis functions", *Computational Mechanics*, Vol. 26 No. 4, pp. 333-43.

Further reading

Murakami, A. and Arimoto, S. (2003), "Localized behavior of saturated soil via element-free strategy", *Proceedings of 12th Asian Regional Conference on Soil Mechanics and Geotechnical Engineering*, Vol. 1, pp. 925-8.